Journal of Maps

ISSN: (Print) 1744-5647 (Online) Journal homepage: http://www.tandfonline.com/loi/tjom20

The Mount Pizzuto earth flow: deformational pattern and recent thrusting evolution

Luigi Guerriero, Paola Revellino, Alessio Luongo, Mariano Focareta, Gerardo Grelle & Francesco M. Guadagno

To cite this article: Luigi Guerriero, Paola Revellino, Alessio Luongo, Mariano Focareta, Gerardo Grelle & Francesco M. Guadagno (2016) The Mount Pizzuto earth flow: deformational pattern and recent thrusting evolution, Journal of Maps, 12:5, 1187-1194, DOI: 10.1080/17445647.2016.1145150

To link to this article: https://doi.org/10.1080/17445647.2016.1145150

JOURNAL OF MAPS, 2016
VOL. 12, NO. 5, 1187–1194
http://dx.doi.org/10.1080/17445647.2016.1145150

Taylor & Francis
Taylor & Francis Group

SCIENCE

The Mount Pizzuto earth flow: deformational pattern and recent thrusting evolution

Luigi Guerriero[a], Paola Revellino[a], Alessio Luongo[a], Mariano Focareta[b], Gerardo Grelle[a] and Francesco M. Guadagno[a]

[a]Department of Sciences and Technologies, University of Sannio, Benevento, Italy; [b]MARSec, Mediterranean Agency for Remote Sensing and Environmental Control, Benevento, Italy

ABSTRACT

The Mount Pizzuto earth flow has been periodically active in recent decades. Early in 2006, it surged and created a dam across the Ginestra torrent. Episodic floods induced by the earth-flow dam periodically damaged a section of a local road and power and telephone service lines. This paper presents a map showing deformational structures along the flow and a geometric reconstruction of thrust faults at the earth-flow toe from 2006 to 2014. The map, produced on the basis of field observations, shows the spatial distribution of back-tilted surfaces, flank ridges and normal, thrust, and strike-slip faults. Springs, creeks, and ponds are also shown on the map. The map indicates that the earth flow is composed of five kinematic zones. Cartographic data and the spatial–temporal reconstruction of the thrusting evolution offer the basis for interpreting the (mid-term) kinematics of the flow and its controlling factors, and for assessing the influence of earth-flow movement on torrent channel capacity.

ARTICLE HISTORY
Received 15 June 2015
Revised 21 October 2015
Accepted 19 January 2016

KEYWORDS
Earth flow; structure; deformation; kinematics; Italy

1. Introduction

Earth flows (Varnes, 1978) are the dominant erosion mechanism in many mountainous landscapes and are among the most common mass-movement phenomena in nature (Keefer & Johnson, 1983; Mackey, Roering, & McKean, 2009). They generally involve fine-grained sediments and in favorable geologic conditions can affect large areas (e.g. Guerriero, Revellino, Coe et al., 2013; Guerriero, Revellino, Grelle et al., 2013; Guerriero et al., 2014; Guerriero, Diodato, et al., 2015; Guerriero, Revellino, et al., 2015). In southern Italy, the majority of active earth flows are reactivations of ancient earth-flow deposits; they are a common feature where structurally complex geologic formations form relief (Grelle, Revellino, Donnarumma, & Guadagno, 2011; Grelle, Soriano, et al., 2014). Approximately 46% of Benevento province (southern Italy) is affected by earth flows and 40% of these slope movements involve an area larger than 0.1 km^2 (Donnarumma, Revellino, Grelle, & Guadagno, 2013; Revellino, Grelle, Donnarumma, & Guadagno, 2010).

Among the most active earth flows of Benevento province is the Mount Pizzuto earth flow (Figure 2 in the Main Map). It affects the northeastern side of the Pizzuto Mount from approximately 720 m a.s.l. to approximately 550 m a.s.l., and involves an estimated volume of approximately 300,000 m^3 of fine-grained flyschoid material. From a geological perspective, the earth flow is located at the overthrust fault between (i) the Argille Varicolori formation: this consists of a sequence of polychrome clays or argillites that form the upper part of the slope, where the flow source area is located and (ii) the Flysch of San Bartolomeo formation: this is formed by terrigenous and turbiditic deposits, outcropping in the middle and lower parts of the slope (Pescatore, Di Nocera, Matano, & Pinto, 2000). The tectonic contact between the two formations materializes in a west northwest-east southeast trending thrust fault that constitutes a weak zone where several landslide source areas are localized (Pescatore et al., 2000).

The Mount Pizzuto earth flow has been periodically active in recent decades and early in 2006 it surged damming the Ginestra torrent at its toe. The earth-flow dam induced several floods that periodically damaged a section of a local road and power and telephone service lines. In 2008, a ditch was excavated along the torrent and a large diameter drain was installed. It worked until early 2011, when a new flood destroyed the drain, the local road, and the service lines.

Recent research has revealed that large earth flows can be decomposed into several quasi-discrete kinematic zones that operate in unison to transmit pulses of sediment along the length of the flow (Guerriero et al., 2014). A kinematic zone (Figure 1; e.g. Guerriero et al., 2014) can be defined as a sector of the earth flow characterized by an area of stretching with one or more normal faults at its head (i.e. a driving element) and an area of shortening with one or more back-tilted

CONTACT Luigi Guerriero luigi.guerriero@unisannio.it

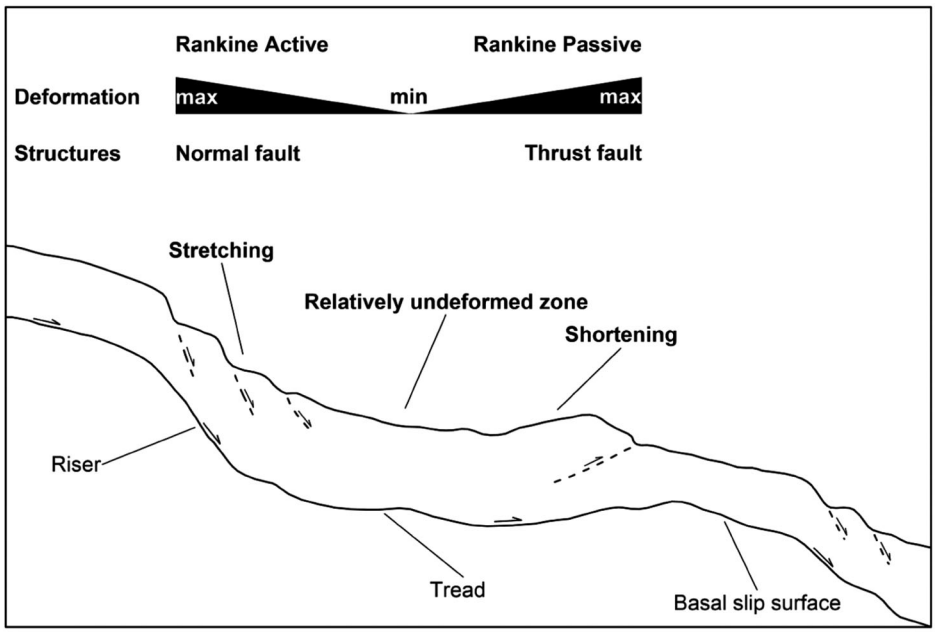

Figure 1 . Schematic longitudinal profile of a kinematic zone. (for further details see Guerriero et al., 2014)

surfaces or thrust faults at its toe (resisting elements). In some cases, the kinematic zones of the Pizzuto earth flow had a central area of no stretching or shortening where earth-flow movement occurred largely by translation along discrete basal- and lateral-slip surfaces.

As a first step, toward gaining a better understanding of the style and evolution of the movement and earth-flow segmentation, we (i) mapped deformational structures and hydrologic features (i.e. creeks, springs, and ponds) in September 2014 and (ii) tracked the thrusting evolution at the earth-flow toe from 2006 to 2014 via field mapping and the interpretation of multi-temporal aerial images. Mapping of deformational and hydrologic features on similar earth flows in Colorado and Italy has shown that they can be used to identify kinematic elements within the earth flow and hydrologic features can be used to infer the geometry of the basal-slip surface (Baum & Fleming, 1991; Coe, McKenna, Godt, & Baum, 2009). Our map (Main Map) and thrusting analysis provide a basis for interpreting the kinematics of the Mount Pizzuto earth flow and its influence on the channel capacity of the Ginestra torrent. Such an interpretation will be provided in a forthcoming paper.

Figure 2. The Head of the Mount Pizzuto earth flow on 13 October 2014.

2. Mapping methods

The map of the Mount Pizzuto earth flow was produced on the basis of data acquired during 11 field visits, completed in September 2014. The cartographic elements were mapped using the real-time kinematic (RTK) global positioning system (GPS) technique (e.g. Gili, Corominas, & Rius, 2000), specifically a Leica Viva Net dual-frequency receiver. The horizontal accuracy ranged between ±1.5 and ±7.2 cm; vertical accuracy ranged between ±3 and ±11.2 cm. GPS data were exported in the form of vector features as points, lines, and polygons, and were processed in a geographical information system (GIS). We used terminology and classifications from structural geology to describe the deformational structures within the earth flow because they accurately depict the geometry and relative sense of displacements of the structures observed (e.g. Guerriero, Revellino, Coe et al., 2013). Surface deformational features such as back-tilted surfaces, flank ridges, and faults are expressions of local variations in earth-flow speed, volume, boundary geometry (Fleming, Baum, & Giardino, 1999; Fleming & Johnson, 1989; Guerriero et al., 2014; Parise, 2003), variations in the mechanical strengths of the materials, and driving and resisting elements within earth flows (Baum & Fleming, 1991). Our map contains the positions of the benchmarks that were installed within the earth flow on 8 April 2014 with the aim of monitoring flow kinematics. The Benchmark survey was carried out using a tripod. The Horizontal accuracy in positioning calculated by our device ranged from ±0.7 cm to ±1.6 cm.

We defined major kinematic zones (or elements) on the basis of the mapped distribution of the structures. In particular, major groups of normal faults identify major driving earth-flow elements while groups of thrust faults, locally associated with folds and back-tilted surfaces, identify resisting earth-flow elements (Baum & Fleming, 1991). Paired driving and resisting elements form a kinematic zone. Areas of transition between the kinematic zones (i.e. limits) were established between the lower thrust fault of the upper zone and the upper normal fault of the lower zone. It is important to note that kinematic element limits, simplified in the Main Map as lines, have to be considered as volumes.

The thrusting evolution at the earth-flow toe was tracked via the multi-temporal mapping of the thrust faults from 2006 to 2014. Thrust-fault mapping was completed using both field mapping and photo interpretation (e.g. Keaton & Degraff, 1996). In October 2006, thrust faults were mapped via the visual interpretation of a color orthophoto. In April 2011, thrust faults were mapped via the visual interpretation of a Google Earth color orthoimage. In September 2008 and July 2014, thrust faults were mapped in the field using RTK GPS (e.g. Gili et al., 2000). Horizontal accuracy during the July 2008 campaign was approximately ±2 cm; 3D accuracy was approximately ±4.5 cm.

3. Results

3.1. Deformational pattern and segmentation

Deformational structures within the Mount Pizzuto earth flow comprise normal faults and tension cracks, indicating earth-flow stretching, thrust faults, flank ridges, fold structures, and pressure ridges indicating earth-flow shortening and back-tilted surfaces indicating backward rotation and strike-slip faults bounding the earth-flow moving core. Five kinematic zones were recognized along the earth flow (Main Map): the Head, the Hopper, the Neck, the Body, and the Toe.

The Head (Figure 2) is formed by two coalescent branches. The northern branch is approximately 230 m long while the length of the southern branch is approximately 160 m long. The width of the northern branch ranges between 9.5 and 30 m and the width of the southern branch ranges between 7.5 and 16 m.

The northern branch begins with a group of normal faults delineating a natural amphitheater. Such normal faults define the upper bound of the main head-scarp. Its height ranges from 3 to 4 m. In these parts of the flow, the moving core is laterally bounded by normal faults locally associated with sets of en-echelon tension cracks. Downslope from this first set of normal faults, the earth-flow moving core is bounded by discontinuous strike-slip faults. Segments of strike-slip faults are arranged as left- or right-stepping en-echelon arrays and the stepping direction controls the width of the earth flow. For example, in the upper zone, strike-slip segments step inward narrowing the earth flow. From 680 m a.s.l., segments step outward widening the flow section. Segment lengths range from 4 to 30 m. From 705 to 665 m a.s.l., there are three groups of normal faults indicating a stretching of earth-flow material. Between the first (around benchmark no. 1) and the second (downslope from benchmark no. 2) groups are thrust faults indicating local shortening of the flow. A shallow landslide with a normal fault at its head and a thrust fault at its toe is located external to the left flank of the earth-flow moving core. Downslope from the lower group of the normal faults, where the slope angle ranges from 15° to 10°, a group of tension cracks indicate stretching of earth-flow material (around benchmark no. 4). Downslope from this group of tension cracks, an association of thrust faults, pressure ridge, and back-tilted surfaces indicates shortening of earth-flow material. Back-tilted surfaces contain ponds.

Similar to the northern branch, the southern branch begins with a group of normal faults delineating a smaller amphitheater forming the main head-scarp

(from 2 to 4 m high). In this part of the flow, around benchmark no. 8, the moving core is laterally bounded by normal faults. Downslope from this first group of normal faults, the earth flow is bounded by strike-slip faults. Several normal faults indicate stretching in the upper zone of this branch. Downslope from the normal faults, a thrust fault is associated with a larger back-tilted surface and two smaller back-tilted surfaces containing two ponds. Downslope from benchmark no. 6, three groups of tension cracks indicate stretching along the flow and a back-tilted surface is present near the right flank in an almost flat zone at approximately 660 m a.s.l. Downslope from this back-tilted surface and from the lowest group of tension cracks, thrust faults indicate shortening of earth-flow material. In this zone, where the Head kinematic zone ends, the northern and the southern branches join (Figure 3 in the Main Map).

Downslope from the Head zone, a highly fractured area (Figure 3) marks the beginning of the Hopper kinematic zone (Figure 4). This kinematic zone is approximately 115 m long and its width ranges from 45 m in its upper part to 32 m of its lower part. It is laterally bounded by inward-stepping strike-slip faults, whose lengths range from less than 2 m to approximately 20 m. Such faults, accommodating earth-flow narrowing, are locally associated with en-echelon sets of tension cracks and near the end of the zone are associated with flank ridges. The earth-flow Hopper can be divided into three major zones. The upper zone is characterized by an upper and a lower highly fractured area with a group of normal faults in the middle (from benchmark no. 9 to benchmark no. 13, along the longitudinal axis of the flow). The lower zone is characterized by thrust faults associated with back-tilted surfaces containing ponds (around

Figure 3. The transition zone between the earth-flow Head and the earth-flow Hopper kinematic zones.

Figure 4. The earth-flow Hopper on 29 March 2014.

benchmarks no. 16 and no. 17). Between these zones, a middle zone contains a group of normal faults that face downslope in their upper part and tend to face toward the flanks in the lower part.

Around benchmark no. 18 begins the Neck kinematic zone. This kinematic zone contains the earth-flow neck, the narrowest section of the earth flow, shown in Figure 1 of the Main Map. The Neck is approximately 130 m long and its width ranges from approximately 30 m in the upper section to less than 10 m. Along the Neck, the moving core is bounded on both flanks by discontinuous strike-slip faults that step inward upslope from the neck and outward downslope. It begins with a highly fractured area that evolves downslope into a cluster of downslope-facing normal faults. Near benchmark no. 21, thrust faults facing toward the flanks are associated with lateral ridges (Figure 5). The narrowest section of the flow corresponds to an area of normal faulting. During the last surge in April 2014, the neck was exposed, permitting the observation of its geometry (Figure 1 of Main Map). The Neck kinematic zone ends at 610 m a.s.l.

Figure 5. Flank ridge forming the left flank of the earth flow on 7 November 2014.

corresponding to the thrust faults. In April 2014, such thrust faults were associated with a back-tilted surface containing a pond (Figure 6).

Downslope from the Neck is the Body kinematic zone. It is approximately 240 m long and segments of the strike-slip faults, locally alternating with en-echelon sets of tension cracks, form earth-flow flanks. Over such a distance, the earth flow widens from approximately 14 m to approximately 40 m. In the upper part of the Body, a set of tension cracks and two groups of normal faults are the result of material stretching. Around benchmark no. 25, a thrust fault indicates local shortening. Downslope, two clusters of normal faults indicate stretching of the earth-flow material. A first right step in the right flank at approximately 589 m a.s.l. widens the earth flow by approximately 5 m and a pull-apart basin is present. This structural depression is associated with a bend in the lateral faults that tends to enlarge the earth flow and contains both extensional and compressional structures. Especially at 590 m a.s.l., a group of upslope- and downslope-dipping normal faults accommodate material migration toward the depression. Within the depression, a thrust fault and an en-echelon set of tension cracks indicate shortening and stretching of outgoing earth-flow material. Orientation of extensional and compressional structures at the step in earth-flow flank seems to indicate a planar rotation of the material induced by the presence of the structural basin. Downslope from this first structural basin, the presence of a downslope-dipping group of normal faults and an upslope-dipping group of normal faults can also be connected to the planar rotation of the sliding material. Such a rotation should depend on the presence of a second, larger, pull-apart basin. Normal faults and tension cracks indicate a downslope extension toward the basin. Within the structural depression, a thrust fault and a fold structure are present. Downslope, a 30 m longitudinal thrust and several segments of thrust fault form the suture line between the material remobilized in April 2014 and the material outgoing from the structural basin. Lateral thrusting causes a reduction of the section of the April 2014 earth-flow creek (Figure 3 in the Main Map). North of this thrust, a normal fault accommodates stretching toward the thrust. Along the right flank, a third, larger, pull-apart basin is developed at approximately 570 m a.s.l. Thrust faults, fold structures, and lateral segments of strike-slip faults delineate this basin. Upslope, extension of earth-flow material toward the basin is accommodated by upslope and downslope-facing normal faults. Material outgoing from the basin is affected by tension cracks. Thrust faults in this part of the earth flow mark the end of the Body kinematic zone.

At 570 m a.s.l. a group of normal faults (upslope from benchmark no. 28) delineates the beginning of the Toe kinematic zone. It is approximately 200 m long and reaches about 150 m wide at the thrust forming the lower end of the earth flow where earth-flow material is spread out toward the Ginestra torrent. The earth flow Toe consists of a smaller, upper, extensional zone with a group of normal faults, and a larger compressional zone with large thrust faults associated with back-tilted surfaces. Most of these back-tilted surfaces contain ponds. Locally on the ground surface, an association of normal faults creating grabens are

Figure 6. Back-tilted surface containing a pond associated with thrust fault delineating the end of the Neck kinematic zone on 29 March 2014.

recognizable. Moreover, the distal part of the earth-flow Toe is affected by shallow landslides. Such landslides transfer earth-flow material toward the Ginestra torrent.

The earth-flow hydrographic network begins at 693 m a.s.l. where a spring is associated with a thrust fault along the northern branch of the Head kinematic zone. In this part of the flow, the creek is a V-shaped channel connected with the largest pond of the lower sector of the Head. The presence and persistence of this pond is probably caused by inflow in the back-tilted surface and the absence of an outflow channel (e.g. Coe et al., 2009). In the southern part of the Head, a spring associated with a thrust fault feeds the earth flow creek. This V-shaped creek is located along the right flank of the flow in the upper part of the Hopper and tends to develop along the longitudinal axis of the flow downslope, until the earth-flow neck. Around benchmark no. 19, a second creek fed by a pond located downslope from a thrust fault contributes to supplying water to the channel. Downslope from the neck, the earth flow creek is located along the right flank following steps in lateral boundaries and pull-apart depressions. Downslope from the lowest structural basin, the creek migrates toward the north, feeding a pond located within a back-tilted surface. Downslope from this pond, the creek develops toward the northeast reaching the Ginestra torrent. At 570 m a.s.l., along the right flank, a spring feeds another creek that follows the right flank of the earth flow reaching the Ginestra torrent. Field observations conducted in 2014 show that water flow within the earth-flow creek was also persistent in the summer.

3.2. Recent thrusting evolution

All of the thrust faults mapped both in the field and through aerial-image interpretation advanced from October 2006 to September 2014 (inset map within the Main Map). An exception is the distal thrust fault delineating the lower end of the earth flow, which negligibly changed its location and geometry with the advancing earth flow and failure progression. This thrust fault was located within the bed of the Ginestra torrent and was influenced by fluvial activity (i.e. erosion).

The geometry and position of the four groups of the advancing thrust faults are shown on the inset map within the Main Map along with the corresponding mapping dates. The line pattern corresponds to a specific date. Thrust-fault advancement was not constant and the thrust geometry changed over time. For example, along their paths, the red thrust fault advanced from 20 to 26 m and the purple thrust fault advanced from 40 to 45 m. The red thrust fault conserved most of its original geometry during the thrust evolution. In contrast, the green thrust fault moved forward from 20 to 30 m and the yellow thrust fault advanced by approximately 30 m. In these two last cases, the original geometry was not maintained during the observation period.

4. Conclusions

The Mount Pizzuto earth flow surged in 2006 when it dammed the Ginestra torrent inducing episodic floods that destroyed local infrastructure and service lines. Its activity and effects on the local hydrographic network make the landslide a very interesting natural laboratory for mid-term monitoring of earth-flow kinematics and the effects of an earth flow on torrent channel capacity. Our map indicates that the earth flow is a repeating series of driving (i.e. extending flow, stretching) and resisting elements (i.e. compressive flow, shortening) and is composed of five quasi-discrete kinematic zones that operate in unison to transmit a sediment pulse along the flow. Data contained on our map (i.e. style and position of deformational structures) as well as thrust fault geometry and displacement will be used to supplement an interpretation of earth-flow kinematics and can form the basis for an evaluation of the influence of earth-flow movement on torrent channel capacity.

Software

The map was produced using Golden Software Map Viewer 8. GPS data were processed using the Quantum GIS.

Acknowledgements

We would like to thank Francisco Gutiérrez, Marten Geertsema, and Chris Orton for their constructive reviews of this paper.

Disclosure statement

No potential conflict of interest was reported by the authors.

Funding

This paper was financed by PRIN 2010–2011 ([project 2010E89BPY_001] national coordinator: F.M. Guadagno).

ORCID

Luigi Guerriero http://orcid.org/0000-0002-5837-5409
Paola Revellino http://orcid.org/0000-0001-8303-8407
Gerardo Grelle http://orcid.org/0000-0003-1128-5745

Francesco M. Guadagno http://orcid.org/0000-0001-5195-3758

References

Baum, R. L., & Fleming, R. W. (1991). Use of longitudinal strain in identifying driving and resisting elements of landslides. *Geological Society of America Bulletin*, *103*, 1121–1132.

Coe, J. A., McKenna, J. P., Godt, J. W., & Baum, R. L. (2009). Basal-topographic control of stationary ponds on a continuously moving landslide. *Earth Surface Processes and Landforms*, *34*, 264–279.

Donnarumma, A., Revellino, P., Grelle, G., & Guadagno, F. M. (2013). Slope angle as indicator parameter of landslide susceptibility in a geologically complex area. *Landslide Science and Practice: Landslide Inventory and Susceptibility and Hazard Zoning*, *1*, 425–433.

Fleming, R. W., Baum, R. L., & Giardino, M. (1999). *Map and description of the active part of the Slumgullion Landslide, Hinsdale County, Colorado*. US Geological Survey Miscellaneous Investigation, Series Map I-2672. http://pubs.usgs.gov/imap/i-2672/.

Fleming, R. W., & Johnson, A. M. (1989). Structures associated with strike-slip faults that bound landslide elements. *Engineering Geology*, *27*, 39–114.

Gili, J. A., Corominas, & J., Rius, J. (2000). Using global positioning system techniques in landslide monitoring. *Engineering Geology*, *55*, 167–192.

Grelle, G., Revellino, P., Donnarumma, A., & Guadagno, F. M. (2011). Bedding control on landslides: A methodological approach for computer-aided mapping analysis. *Natural Hazards and Earth System Sciences*, *11*, 1395–1409.

Grelle, G., Soriano, M., Revellino, P., Guerriero, L., Anderson, M. G., Diambra, A. … Guadagno, F. M. (2014). Space-time prediction of rainfall-induced shallow landslides through a combined probabilistic/deterministic approach, optimized for initial water table conditions. *Bulletin of Engineering Geology and the Environment*, *73* (3), 877–890.

Guerriero, L., Coe, J. A., Revellino, P., Grelle, G., Pinto, F., & Guadagno, F. M. (2014). Influence of slip-surface geometry on earth flow deformation, Montaguto earth flow, southern Italy. *Geomorphology*, *219*, 285–305.

Guerriero, L., Diodato, N., Fiorillo, F., Revellino, P., Grelle, G., & Guadagno, F.M. (2015). Reconstruction of long-term earth-flow activity using a hydro-climatological model. *Natural Hazards*, *77*, 1–15.

Guerriero, L., Revellino, P., Coe, J. A., Focareta, M., Grelle, G., Albanese, V., … Guadagno, F. M. (2013). Multi-temporal maps of the Montaguto earth flow in southern Italy from 1954 to 2010. *Journal of Maps*, *9*, 135–145.

Guerriero, L., Revellino, P., Grelle, G., Fiorillo, F., & Guadagno, F.M. (2013). Landslides and Infrastructures: The case of the Montaguto earth flow in Southern Italy. *Italian Journal of Engineering Geology and Environment* (Book Series 6, International Conference Vajont 1963–2013), 447–454.

Guerriero, L., Revellino, P., Mottola, A., Grelle, G., Sappa, G., & Guadagno, F.M. (2015). Multi-temporal mapping of the Caforchio earth flow, southern Italy. *Rendiconti Online della Società Geologica Italiana*, *35*, 166–169.

Keaton, J. R., & Degraff, J. V. (1996). Surface observation and geologic mapping. In A. K. Turner, & R. L. Schuster (eds.), *Land slides investigation and mitigation: Transportation research board special report, 247* (pp. 178–230). Washington, DC: National Academy Press.

Keefer, D.K., & Johnson, A.M. (1983). *Earthflows: morphology, mobilization and movement*. U.S. Geological Survey Professional Paper, 1264, p. 56.

Mackey, B. H., Roering, J. J., & McKean, J. A. (2009). Long-term kinematics and sediment flux of an active earthflow, Eel River, California. *Geology*, *37*(9), 803–806.

Parise, M. (2003). Observation of surface features on an active landslide, and implications for understanding its history of movement. *Natural Hazards and Earth System Sciences*, *3*, 569–580.

Pescatore T., Di Nocera S., Matano F., & Pinto F. (2000). L'unità del Fortore nel quadro della geologia del settore orientale dei Monti del Sannio (Appennino meridionale). *Bollettino della Società Geologica Italiana*, *119*, 587–601.

Revellino, P., Grelle, G., Donnarumma, A., & Guadagno, F. M. (2010). Structurally-controlled earth flows of the Benevento Province (Southern Italy). *Bulletin Engineering Geology and Environment*, *69*, 487–500.

Varnes, D. J. (1978). Slope movement types and processes. In R. L. Schuster, & R. J. Krizek (eds.), *Landslides analysis and control: Transportation research board special report, 176* (pp. 11–33). Washington, DC: National Academy Press.